Water Conservation and Management (WCM)

DOI: http://doi.org/10.26480/wcm.01.2026.95.108

ZIBELINE INTERNATIONAL™ PUBLISHING

ISSN: 2523-5664 (Print)
ISSN: 2523-5672 (Online)
CODEN: WCMABD

CrossMark

RESEARCH ARTICLE

ESTIMATION THE CLIMATE WEATHER INDEXES ON VEGETATION AND WATER REGIONS IN BAGHDAD GOVERNORATE THROUGH ANALYSING HIGH RESOLUTION IMAGERIES USING REMOTE SENSING TECHNOLOGY

Murtadha H. Kareem*, Hayder H. Kareem

Structures and Water Resources Engineering Department, Faculty of Engineering, University of Kufa, Al-Najaf, Iraq
****Corresponding Author Email: murtadhah.aljalihawi@student.uokufa.edu.iq***

Article History:

Received 26 January 2026
Revised 20 February 2026
Accepted 25 February 2026
Available online 05 March 2026

ABSTRACT

Drought constrains agricultural sustainability and ecological viability, especially within arid environments where water resource availability is the fundamental restriction. In this study, we assessed the spatiotemporal variability of droughts and surface water in the Baghdad Governorate State, Iraq using a systematic approach integrating remote sensing and geographic information systems (GIS). A comprehensive series of time-series aerial imagery (Missions 1-9) of the Landsat satellite covering a span of 55 years from 1970-2025 were analyzed at five-year intervals. Two indices were employed: the Vegetation Condition Index (VCI) based on the Normalized Difference Vegetation Index (NDVI) indicative of agricultural stress and the Enhanced Water Index (EWI) used to demarcate Emerged Water Regions (EWR). The analyses demonstrate pronounced cycles of degradation and recovery within this ecosystem. A disastrous 'drought' period was found in 1980 with widespread collapse of vegetation vigor and dramatic contraction of the Tigris and its tributary dry canals. Such extreme deficits were also found in 2000 and 2005, particularly impacting on the agricultural districts of Abu Ghraib and Al-Madain. Hydrogenically speaking, 1995 and additionally 2020 were hydrological 'optimums' where emergent water bodies have directly supported a widespread rejuvenation of lush vegetation. Worryingly perhaps, prediction for 2025 indicates a return to 'Severe' to 'Extreme' level of 'drought' as in the 1980 crisis. Our results provide novel evidence for water managers about the liner dependence of the Baghdad ecosystem on the continuity of surface water relaying grave concerns about the cyclical aridity of the region.

KEYWORDS

VCI, EWI, Drought detection, Landsat Time Series, Emerged Water Region (EWR), Baghdad, Iraq.

1. INTRODUCTION

Surface water resources are critical for ecological balance and economic stability. Global demand for this life sustaining resource is increasingly put under strain by growing human demand in conjunction with the increasing effects of climate change, which is worsening droughts. There is no other place on earth where this is more pronounced than in the Middle East. The region cradle of civilization is naturally arid and is suffering from water shortages partly because of disruption of the Tigris and Euphrates by damming in the upstream countries, culminating in Iraqi suffering - once ancient Mesopotamia. Consequently, water reaching Iraq's floodplain has decreased significantly, accelerating desertification (Nassrullah et al., 2025). If not addressed scientifically, this escalating drought crisis poses severe threats to food security and national economic stability (Riebsame, 2019; Xu et al., 2021). Historical data indicate that drought reduced global agricultural output by over 10% between 1964 and 2007, while the economic costs of climatic disasters rose by more than 30% from 2005 to 2015 due to agricultural impacts (Lesk et al., 2016; FAO, 2018). Despite improved monitoring of climatic factors, rainfall prediction remains uncertain (Lawal et al., 2021). Due to drought and other natural calamities, delayed consequences are hard to quantify. Take precautions to avoid drought research risks (Van Quang et al., 2021). Ecosystems, agriculture, and cities suffer most from drought (Zhang and Jia, 2013). As provide drought severity indexes. Traditional methods include the Palmer Drought Severity Index (PDSI) and the Z-index, which developed to measure soil water depletion, and the Standardized Precipitation Index (SPI), created by (McKee et al., 1993; Ji and Peters, 2003; Palmer, 1965). Although station-based indices offer valuable insights, their spatial coverage is frequently limited, especially in areas characterized by either sparse monitoring networks or considerable topographical diversity (Zhang and Jia, 2013). Remote sensing outperforms ground stations in drought and environmental change detection (Rhee et al., 2010; Sandeep et al., 2021; Wu et al., 2013). Remote sensing often uses VCI—derived from NDVI (Kogan, 1995a; Quiring and Papakryiakou, 2003). VCI measures vegetative health and water stress response, making it a global drought indicator (Gitelson et al., 1998; Kogan, 1997; Shen et al., 2019). Further longitudinal studies substantiate VCI's applicability in different climates. Have used Landsat satellite imagery (1974–2023) to identify past drought periods in Wales and have established the reliability of the VCI in a tropical setting (Vietnam) via its relationship to soil moisture (Kareem, 2024; Thi and Van Hung, 2024). Closer to home, (Taha et al., 2024) have revealed that extreme drought exacerbated by climate change in southern Baghdad (1988–2023) completely devastated farming to the point that there has been 90% conversion to urban or barren land. Although VCI is

Quick Response Code	Access this article online	
	Website: www.watconman.org	**DOI:** 10.26480/wcm.01.2026.95.108

robust, noted its limitations when used in isolation, suggesting composite frameworks for higher precision (Nag et al., 2024). Nevertheless, studies in 2025 continue to demonstrate VCI's capacity to detect localized drought disparities, as seen in Karnataka's Western Ghats, and its ability to monitor ecosystem resilience in Ukraine and Rajasthan (Yadav et al., 2025; Klymenko and Boychenko, 2025; Agarwal et al., 2025). Concurrently, the rapid and reliable extraction of Surface Water Body (SWB) data is essential for managing flood and drought events (Garrido-Rubio et al., 2020; Papa et al., 2022). In arid regions where water availability is threatened by both natural and anthropogenic factors, accurate mapping is critical (Malahlela, 2016). Traditional ground-based methods lack the necessary spatial resolution; thus, the water index method has become the standard in remote sensing (Lu et al., 2021; McFeeters, 1996; Vinayaraj et al., 2018). While the Normalized Difference Water Index (NDWI) and its modified version (MNDWI) are foundational for global mapping, they often struggle to distinguish water from urban features (Allen and Pavelsky, 2018; Yamazaki et al., 2015). Despite lowering vegetative signals, the NDWI sometimes confuses water with urban characteristics. MNDWI SWIR bands diminish soil reflectance and building shadows (Allen and Pavelsky, 2018; McFeeters, 1996). To mitigate this, the Enhanced Water Index (EWI) utilizes specific band combinations to filter atmospheric interference, and localized indices such as the WI2006, designed for wetland evaluation (Yan, 2007; Danaher and Collett, 2006). Recent applications affirm EWI's efficacy. As employed EWI with Landsat data (1974–2023) to identify long-term hydrological cycles in Cardiff, UK (Kareem et al., 2023). Furthermore, as urbanization complicates water extraction, studies have highlighted the need for advanced indices like EWI integrated with machine learning to improve accuracy in complex terrains by (Purnam et al., 2024; Xia and Lv, 2024). Similarly, demonstrated that hybrid classification models incorporating EWI effectively monitor seasonal water body dynamics in rapidly urbanizing cities like Zhengzhou (Song et al., 2025). The purpose of this research is to assess, investigate, and describe agricultural drought in the Baghdad Governorate through the application of a rigorous analysis of aerial time-series data. Landsat images (MSS, TM, ETM+, OLI) were downloaded for the period extending from 1970 to 2025, at 5-year intervals, to build an integrated picture of the spatial and temporal dynamics of drought and its cumulative effects on land cover. The Vegetation Condition Index (VCI) will be utilized to reduce the impact of geographical differences in vegetation, while the Enhanced Water Index (EWI) will be detected to obtain precise water body information. By classifying these indices into various categories, this study aims to evaluate the incidence of drought and identify severe hotspots within the governorate. The findings provide critical implications for science-based water resource management, assisting researchers in understanding the region's persistence and shifting surface-water fluctuations.

2. Study Area

The Baghdad Governorate is located within the Mesopotamian alluvial plain in the center of Iraq, encompassing the political and economic capital city of Iraq. The capital is located within coordinates 33°10'N–33°27′N and 44°10'E–44°33'E, where the Tigris River bifurcates the metropolis into two sectors of Karkh and Rusafa (Haitham et al., 2024; Hashim et al., 2022; Nassrullah et al., 2025; Tawfik and Al-Lami, 2025). It is a low-lying (between 30 and 35 m above sea level), flat area allowing easy lateral extension of the city but causes harbors serious drainage problems (Al-Adili, 1998; Nassrullah et al., 2025). Extensively comprising Quaternary soil deposits of silty and sandy clay; while these soils are valued at their high holding capacity especially in sustaining water, salt has present accumulated in excess and wells approach the surface water – where poorly drained, this adversely affects vegetation indices (Ali and Muhaimeed, 2016; Jassim and Goff, 2006; Taha et al., 2024). Climate of the city is arid to semi-arid subtropical (BWh), with very severe summers (>50 °C) and great evapotranspiration within short winters with rains (100-to 152mm served (Hashim et al., 2022; Tawfik and Al-Lami, 2025). The mean temperature taken from the last forty years recorded proves an increase of 0.86 °, rainfalls have volume followed down by 48 mm but aggravated by UHI, and significant reduction in the flow of Tigris and ultimately quality sells out polymer reports with the system of pollution resubmission (Hashim et al., 2022; Taha et al., 2024). (Al-Ansari et al., 2012; Nassrullah et al., 2025; Taha et al., 2024). The environment also supports a population conglomerated of 8.34 million people and of natural residential suburbs which dramatically expanded to 41% of there were between 1984 to 2020 respectively 3 (Haitham et al., 2024; Hashim et al., 2022). The impact is particularly pronounced in Southern Baghdad, where 90% of land was converted to be impervious by urbanization and drought, intensifying the UHI and resulting in difficult spectral environments that Index's must be developed (Taha et al., 2024; Tawfik and Al-Lami, 2025; Haitham et al., 2024).

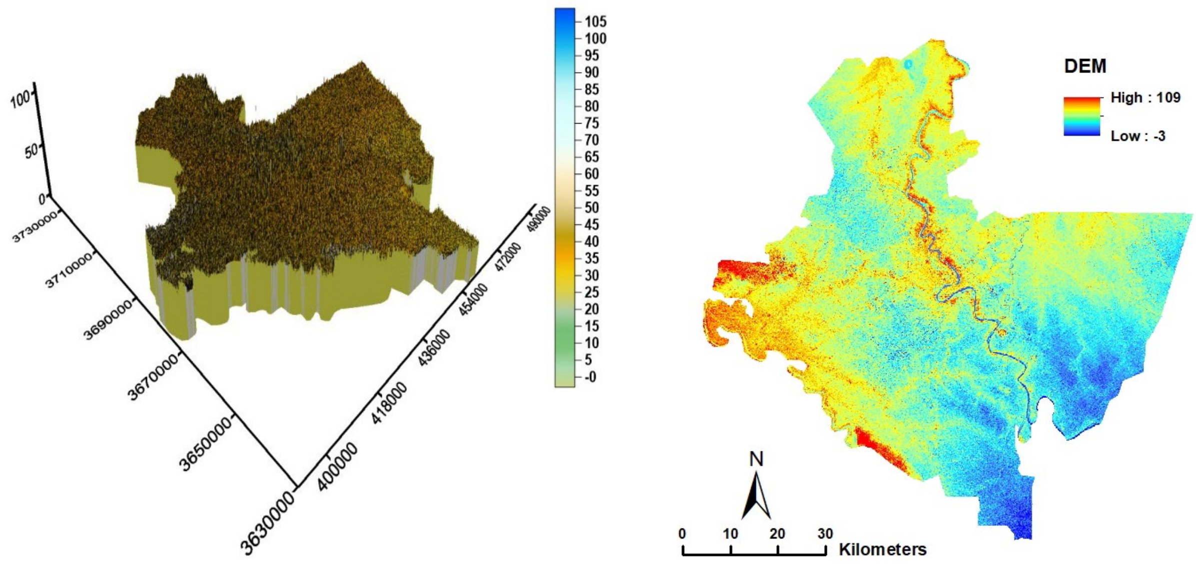

Figure 1: The DEM with a 3D sketch of Baghdad City, Iraq

2.1 Programs and websites used

A framework of environmental monitoring of events such as drought is achievable through the integration of remote sensing data with GIS. This paper adheres to a uniform approach, starting with the acquisition of good quality ortho-rectified satellite images from US Geological Survey (USGS) Earth Explorer , an archive where the "Landsat" datasets used to detail the changing land-use and classification and surface temperature of Earth is stored (Ali and Muhaimeed, 2016; Hashim et al., 2022). We selected multispectral images based on spatiotemporal parameters and derived metadata of the bands needed to determine the spatial secure, long multi-decadal assessment of drought (Taha et al., 2024). ArcGIS (ESRI) thus became the "workhorse" of the paper. The raster datasets were integrated, geometric corrections were performed before conducting plays pace to assess the precise classification of land (Haitham et al., 2024). The analysis made use of the built-in tools in ArcGIS that conferred the ability to delineate effective maps from satellite imagery (Aznarez et al., 2021). Meanwhile, Layer Stacking made composite images from the monochromatic bands we selected (Kareem et al., 2021, Kareem et al., 2023). The Raster Calculator performed mathematics as it computed statistics needed for the determination of indices. That of the red and near-infrared integration formed the (NDVI) for use by field staff to monitor agriculture's drought here (Nag et al., 2024). Spectral bands also helped with water indices delineating water body surfaces and detailing vegetation stress and water availability (Purnam et al., 2024; Klymenko and Boychenko, 2025).

3. METHODOLOGY

Fundamentally, drought is defined as a prolonged period where precipitation is below average, which causes severe water shortages that have adverse effects on ecosystems and agriculture. Remote sensing provides the best products for assessing environmental stressors such as drought through intensity and geographic distribution. Vegetation Condition Index [VCI] uses satellite spectral reflectance data to quantify the physiological health of both cultivated and native vegetation. The VCI is one of the best ways to separate the weather-related effects, like rainfall anomalies, from the impacts related to plant growth. VCI can indicate plant health and can thus be used to identify vegetative stress from climatic changes, as well as groundwater shortages (Gaznayee et al., 2021; Wenzhe et al., 2016). By using both the VCI and NDVI values, vegetative moisture stress can often be detected prior to visible wilting. In addition to being a key component for tracking the onset of droughts, lower VCI values correlate to reduced water availability and affected plant survival (Senhorelo et al., 2023). Therefore, the VCI is integral to an early warning system for drought detection. VCI is derived using the current vegetation conditions divided by historical vegetation conditions' maximum and minimum values (Kogan, 1995b).

$$VCI = \left[\frac{NDVI - NDVI_{MIN}}{NDVI_{MAX} - NDVI_{MIN}}\right] \times 100 \quad (1)$$

The (VCI) serves as a comparative metric for ecosystem health, where values approaching 100 denote optimal vegetation conditions matching historical peaks. Conversely, values declining toward zero indicate intensifying environmental stress and severe drought. The start of this number is based on the NDVI. NDVI data viewing presence of vegetation

and vigor essencial, is ubiquitous in forest study and in land-use planning. It underlies the main way of reflecting vegetation health and hence allowing the VCI to have a downstream basis. From a spectral viewpoint, NDVI is a crucially insightful tool for the aspects of ecosystem health, ecology and biodiversity. It's sensitive to soil moisture and is effective to outline where it is more arid and to capture desertification. Occasional satellites zoom in on this information from afar to see and monitor climate here; (Gaznayee and Al-Quraishi, 2019) predict outcomes and prevention and fixed location. NDVI using the formula of (Rouse et al., 1974), is considered an essential tool for Water Resource Preparations and conservation.

$$NDVI = \frac{NIR - RED}{NIR + RED} \quad (2)$$

The timing of this analysis dances with meaningful history of change in regional agricultural practices and climate trends in neighboring regions. The first year that Landsat data were acquired was 1972, but 1970 is used as building block of the temporal analysis using 5-year increments - allowing for a holistic record of the slow changes to vegetation from the push and pull of natural and human forces. Technical specifications of the Landsat data used in the analysis can be found in Table 1. All scenes were limited based on availability and presence of clouds (≤ 1% cloud cover) to reduce the impact of atmospheric interference, and images were acquired on dates when the burgeoning wet season yields a healthy mature vegetation signal, represented in spectral analysis of NDVI.

Table 1: Downloaded Landsat of Baghdad City

Satellite	Year	Sensor	Wavelength of used bands (nm)	Spatial resolution (m)	Cloud cover
Landsat-1	1970	MSS	B4 = 0.5 – 0.6 B5 = 0.60–0.70 B6 = 0.7 – 0.8 B7 = 0.8 – 1.1	30	0%
Landsat-2	1975	MSS	B4 = 0.5 – 0.6 B5 = 0.60–0.70 B6 = 0.7 – 0.8 B7 = 0.8 – 1.1	30	0%
Landsat-3	1980	MSS	B4 = 0.5 – 0.6 B5 = 0.60–0.70 B6 = 0.7 – 0.8 B7 = 0.8 – 1.1	30	0%
Landsat-5	1985 1990 1995 2000 2005 2010	TM	B2= 0.52 – 0.60 B3= 0.63–0.69 B4 = 0.76–0.90 B5 = 1.55 –1.75	30	0%
Landsat-8	2015 2020	OLI	B3=0.533 –0.590 B4 = 0.64–0.67 B5 = 0.85–0.88 B6=1.556 – 1.651	30	0%
Landsat-9	2025	OLI-2	B3=0.533 –0.590 B4 = 0.64–0.67 B5 = 0.85–0.88 B6=1.556 – 1.651	30	0%

Analysis of drought duration and severity uses US. Drought Monitor (USDM) classification scheme that suggests that drought events can be categorized by duration, differentiating short-term drought events impacting agriculture and grassland ecology, from long-term impact on hydrology and architecture of ecosystems and ecosystem services that occur even when rainfall returns intermittently. Drought is assigned four levels in increasing severity from "Moderate Drought" through to "Exceptional Drought" and assigns regions "Abnormally Dry" that are developing or returning from aridity to capture other areas in drought. Which integrate USDM (2023) standards with the vegetation health criteria proposed, are detailed in Table 2 by (Kogan, 1990).

Table 2: VCI drought classification	
Drought category	**VCI (%)**
Exceptional drought	0–10
Extreme drought	11–20
Severe drought	21–30
Moderate drought	31–40
Abnormally dry	41–50
Normal or wet conditions	≥50

Following a comprehensive review of water extraction algorithms developed over the past two decades, the (EWI) was selected as the optimal metric for this study. This decision is based on the fact that the EWI has been thoroughly tested within the scientific community for validation against numerous empirical studies, study has demonstrated that the EWI insures a higher suppression of background noise along with correctly identifying water bodies in various geographical terrains and climatic conditions. EWI was used exclusively in this research for reporting surface water features within the study area (Cao et al., 2021; Feyisa et al., 2014). The equation used to calculate is given as

$$EWI = \frac{\gamma Green - \gamma NIR - \gamma MIR}{\gamma Green + \gamma NIR + \gamma MIR} \quad (3)$$

ϒ = band reflectance value where band reflectance subscripts signify the bands used in remote sensing photographs.

Table 1 The technical View of Landsat imagery used for this analysis. The choice of possibility windows was based on strict quality control checks for clarity of image, availability of scene (Path/Row), and strict cloud coverage of less than 1%. Imagery chosen in the discussed windows was specifically chosen for imagery of the phase wet and dry seasons in which phenological maturity of study area vegetation would be attained.

3.1 Landsat Imagery Temporal Processing and Time-Series Analysis

A time-series analysis in contrast to the static benchmarking of land-use or land cover, gives a more aware "time aware" benchmark for monitoring environmental change. Although multi-source data exists, we up to the end prefer single-sensor spectral products mainly due to their greater temporal and spatial consistency (Tariq et al., 2021). For the data gaps in the cloud cover, we would be employing a pixel-based frequency classification method which is expected to yield continuous synthetic images from long sequences (Parente et al., 2019; Somasundaram et al., 2020). The pixel frequency approach is so crucial as it serves analysis of land cover stability in hydro-climatically complex areas. We focus on Baghdad and employ reflectance data from missions 1 to 9 of Landsat spanning 1970 to 2025 at five-year intervals. This multi-decadal time-span routine actually allows (VCI) maps to be derived, and surface water features extracted to determine impacts of drought. We used a labored pre-processing routine to map the spectral bands (Green, Red, NIR, SWIR) across the various sensor generations (MSS, TM, ETM+, OLI) always remembering to benchmark them anyhow. Handy GIS based Composite Band functions were summoned to accurately yield spectral profiles to sensibly and accurately choose our sample points.

The figures illustrate the specific Landsat spectral bands utilized for the analysis.

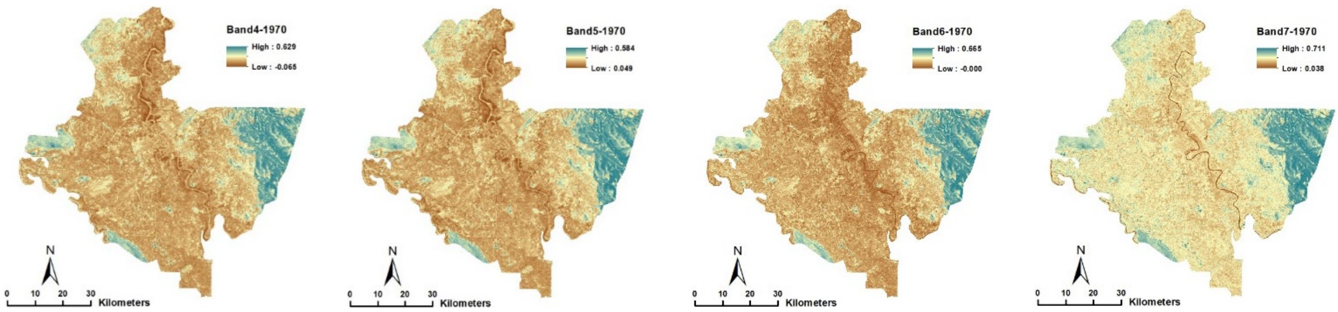

Figure 2 Spectral bands used for the city of Baghdad, Iraq for 1970

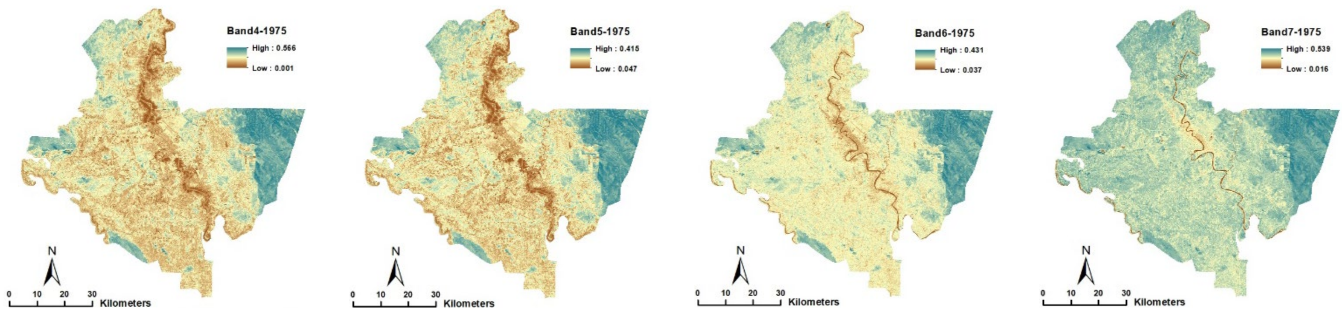

Figure 3 Spectral bands used for the city of Baghdad, Iraq for 1975

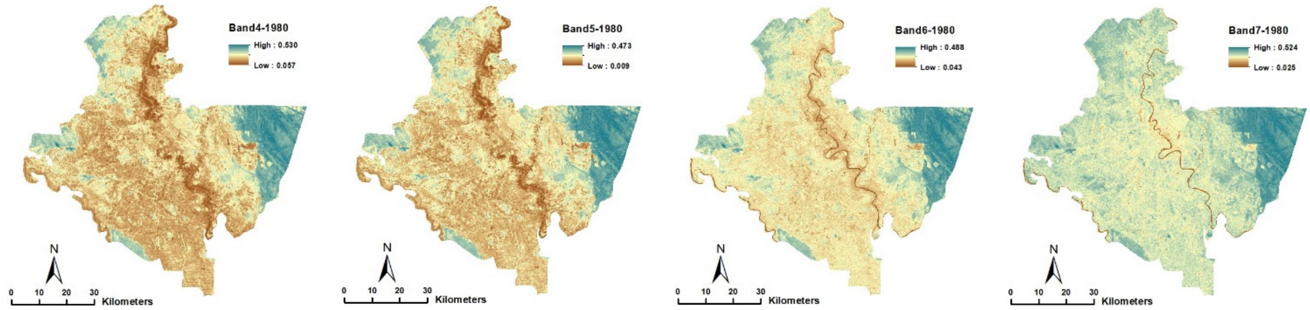

Figure 4 Spectral bands used for the city of Baghdad, Iraq for 1980

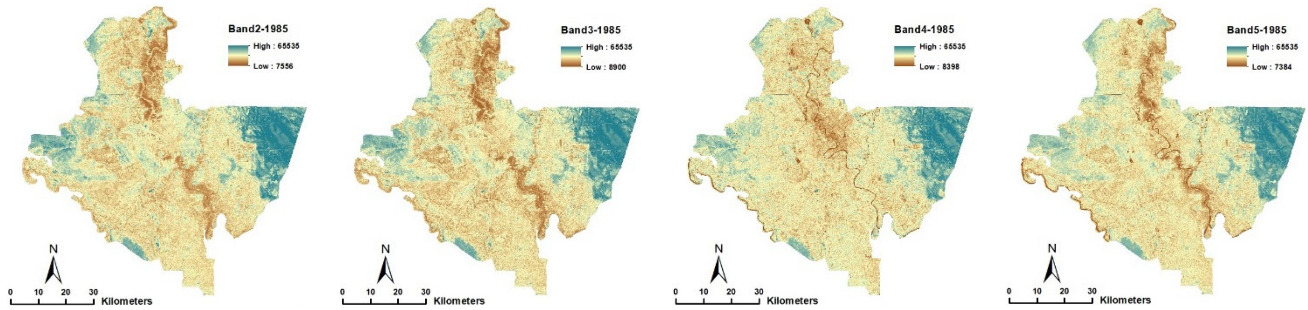

Figure 5 Spectral bands used for the city of Baghdad, Iraq for 1985

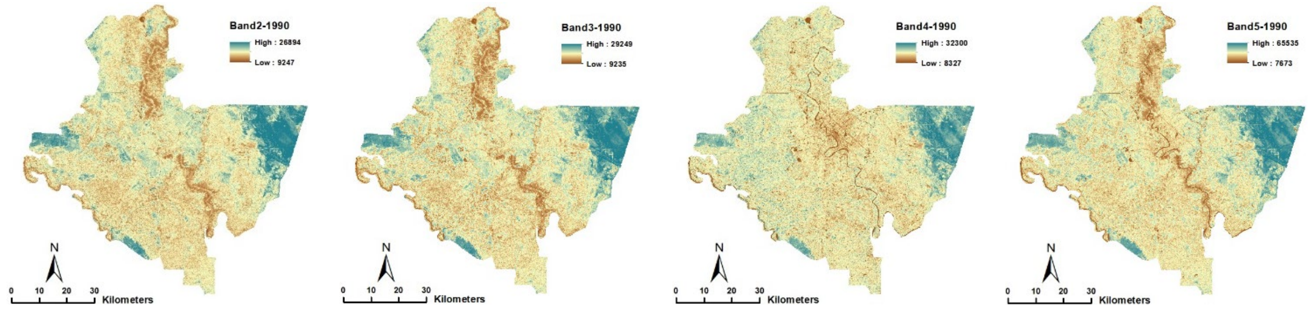

Figure 6 Spectral bands used for the city of Baghdad, Iraq for 1990

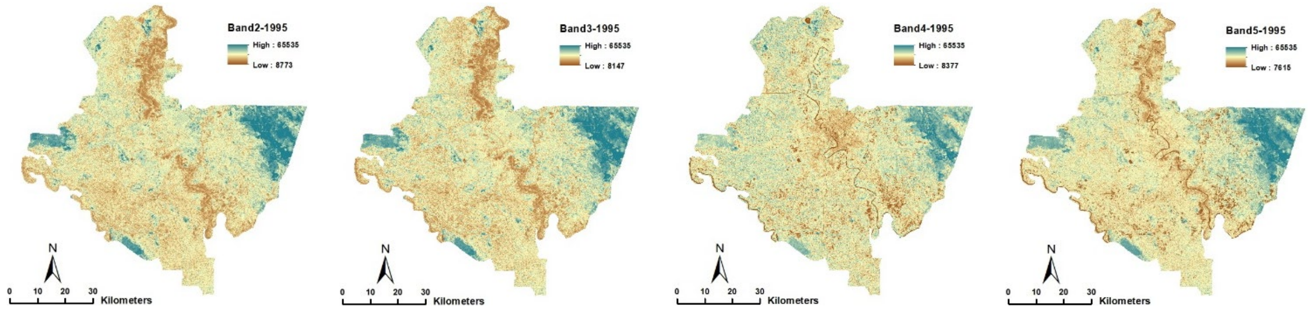

Figure 7 Spectral bands used for the city of Baghdad, Iraq for 1995

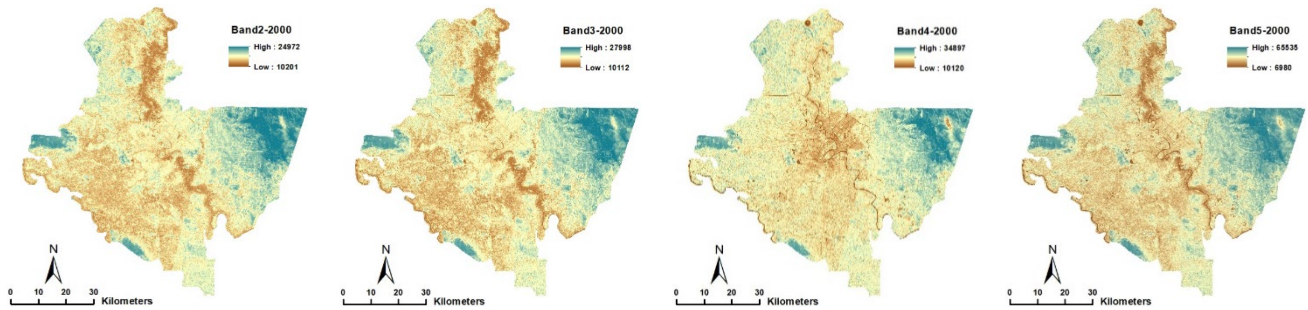

Figure 8 Spectral bands used for the city of Baghdad, Iraq for 2000

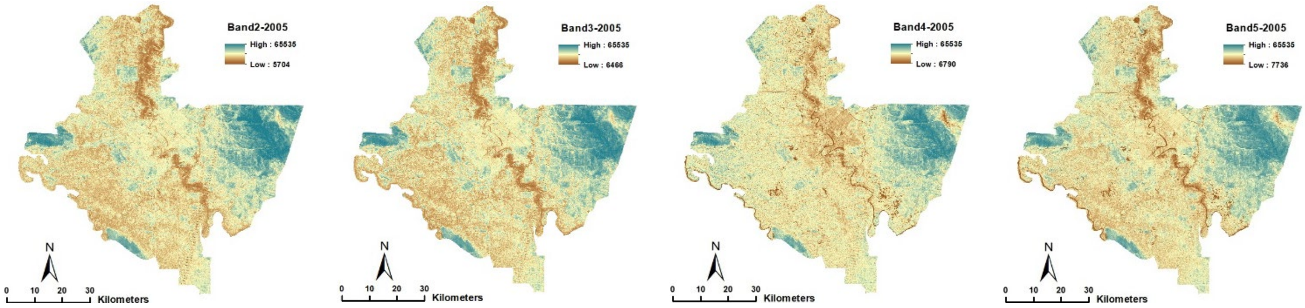

Figure 9 Spectral bands used for the city of Baghdad, Iraq for 2005

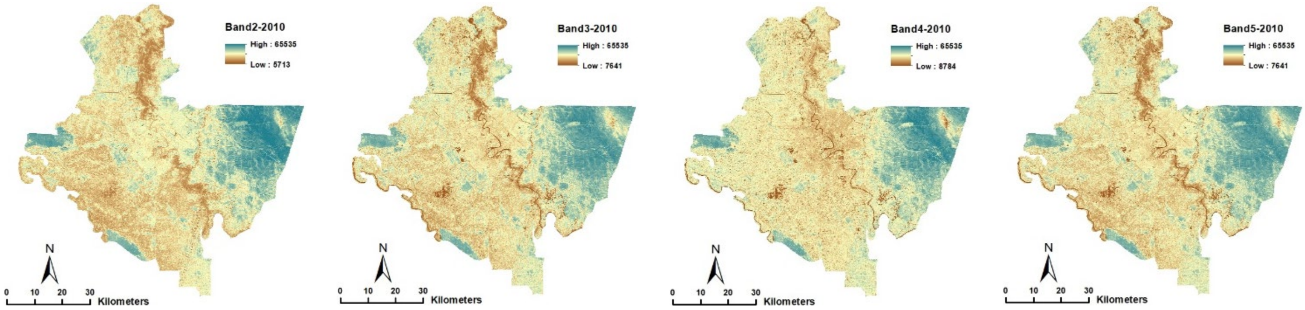

Figure 10 Spectral bands used for the city of Baghdad, Iraq for 2010

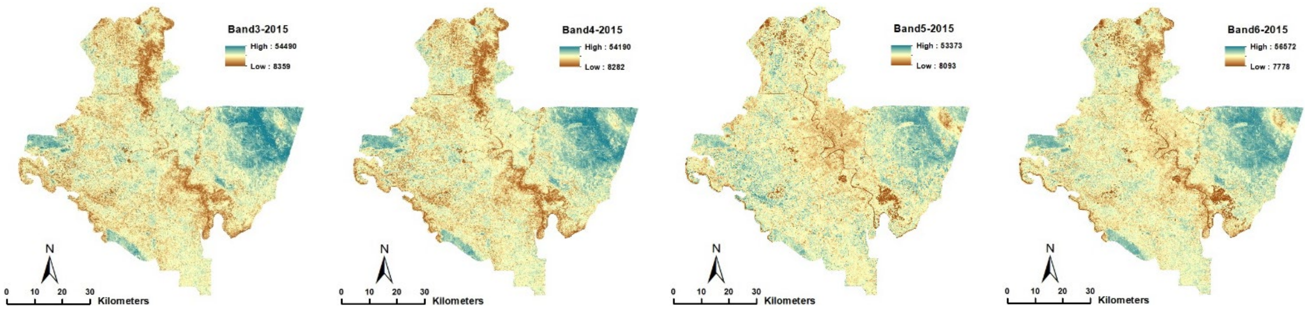

Figure 11 Spectral bands used for the city of Baghdad, Iraq for 2015

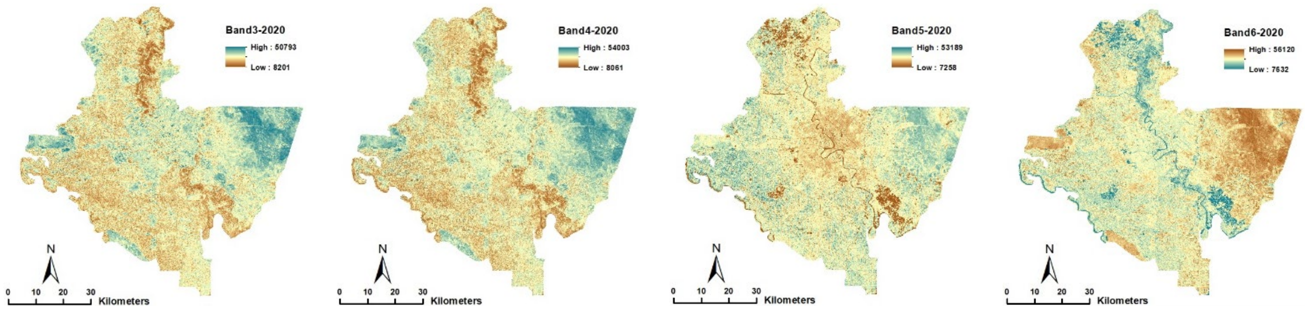

Figure 12 Spectral bands used for the city of Baghdad, Iraq for 2020

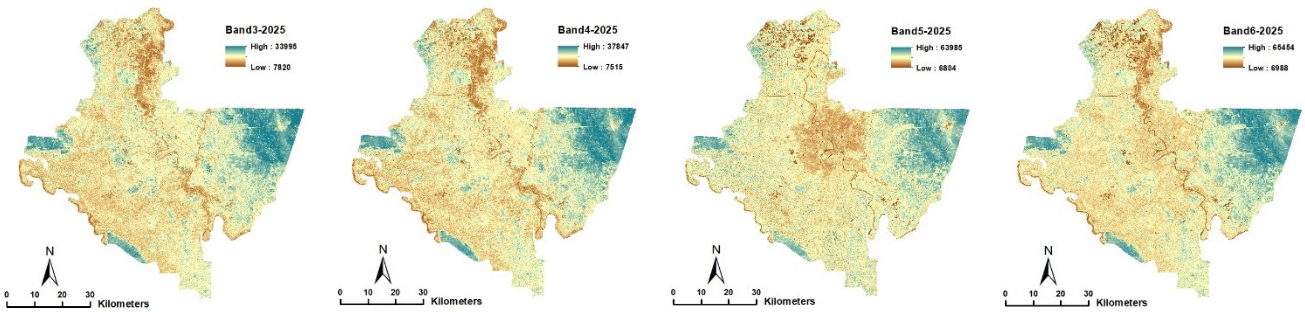

Figure 13 Spectral bands used for the city of Baghdad, Iraq for 2025

The (NDVI) is computed using the unique spectral characteristics of surface elements observed in the visible red and near-infrared (NIR) portions of the electromagnetic spectrum. This index relates to the difference in reflectance between these two spectral bands, yielding a normalized coefficient ranging from -1 to +1. Values approaching +1 demonstrate healthy, green (photosynthesizing) vegetation – the spectral response is the result of red light being absorbed by chlorophyll and NIR radiation being reflected by leaf cell, (and other) tissues. Areas with no vegetation, including built up regions and open water surfaces, will typically assess near zero and negative values. In clear water, where the radiation is absorbed most of the time in both bands, so the return will be negative, though the quality of such water bodies may affect this reaction (Liu et al., 2018) observed elevated Total Suspended Solids (TSS) can change the red and NIR light reflectance, but this spectral signature will still be distinguishable from aquatic and vegetative ones. The images below show the spatio-temporal distribution of (NDVI) for the duration of the study, from 1970 to 2025, five yearly. The images give an insight into the spectral properties of the features of the ground in the study area, which show a close correlation with typical land cover classes' characteristic spectral signatures (think veg, water bodies and urban surfaces, etc.). This validates the sample site selection procedure and also the spectral processing of our multidecadal time series.

1970

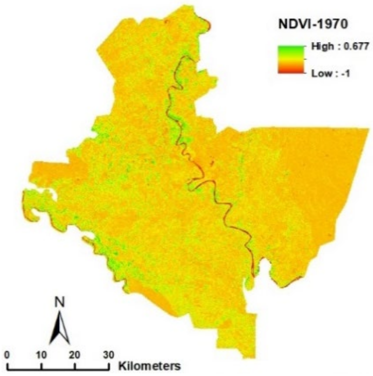

1975

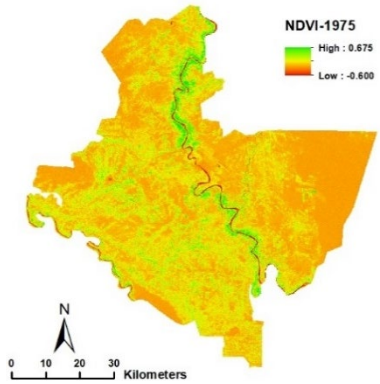

1980

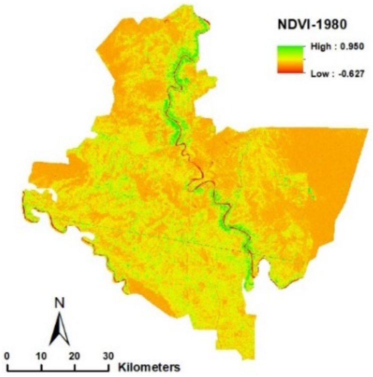

1985

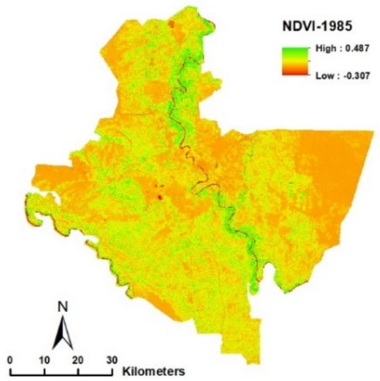

1990

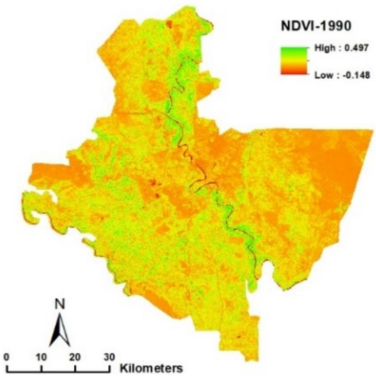

1995

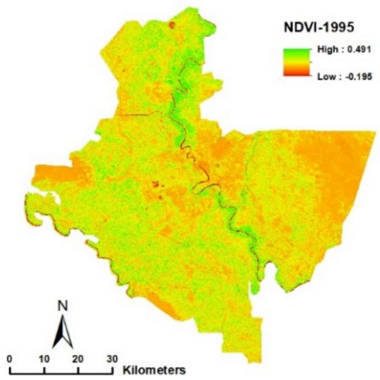

2000

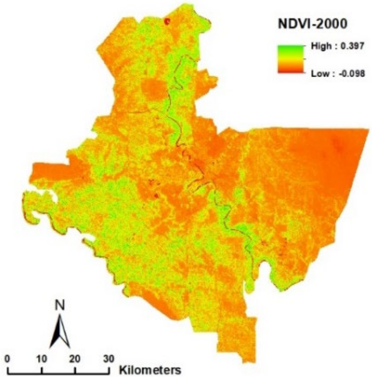

2005

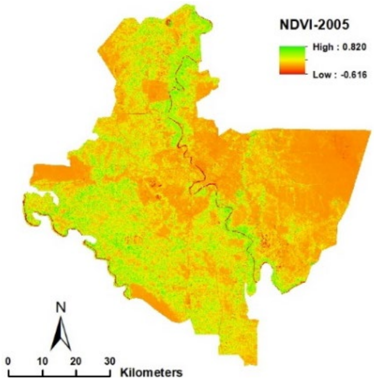

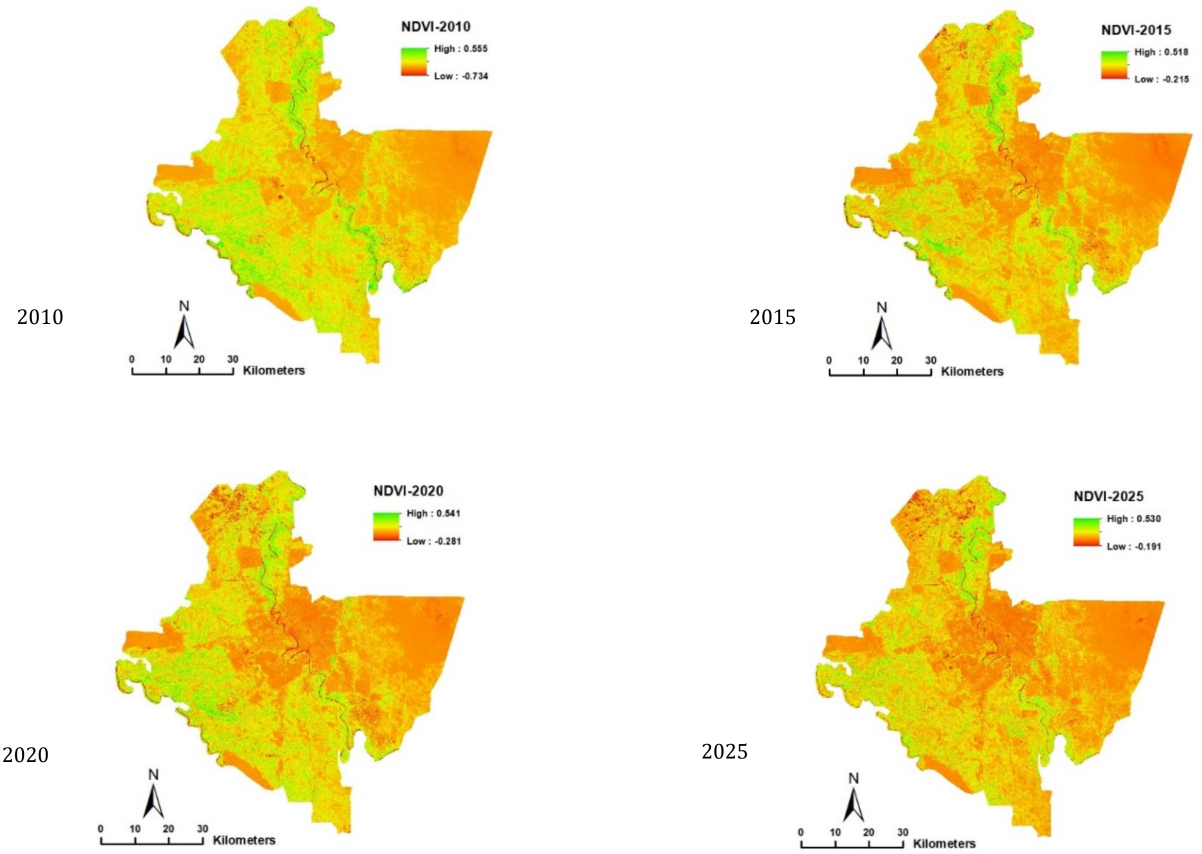

Figure 14: NDVI of Baghdad City, Iraq from 1970 to 2025

4. Results and Analysis

To interpret the drought in our study area we carried the above out for NDVI images that we extracted and processed for years 1970-2025. For this we particularly focus on the meaning of minimum and maximum NDVI for the time series. These metrics are several of the prime metrics for monitoring relative environmental stability and evaluating the health of vegetation over time. For this we need to derive minimum, maximum and average to be able to quantify the behavior of vegetation, in response to environmental and climatic pressure. Stressed vegetation normally tends to grow smaller in domain and also acts less, and less over the landscape. The relative attribute of hosting such vegetation, the mean minimum and maximum hence makes for a good benchmark baseline, as in a field survey on the ground: the vegetation can then be studied from this approach, to inform on where protection efforts should be focused particularly emphasizing their critical points of concern as the vegetation declines for drought. Using the NDVI makes a relatively good gauging tool to streamline agricultural optimization and resource use. Studying the spatial dispersion of healthy and 'weak' vegetation acts to sensitize researchers to drought zones, and ones not prone to medium or low environmental pressure and informing all within the research and public domain about physiologically fit or not fit, sustainable agricultural development, on how to climate switch. The evolution of average minimum and maximum NDVI from our processing of the Landsat time series for 1970-2025 is seen below, Figure 15. All analyses are based on integrated remotes sensing and GIS.

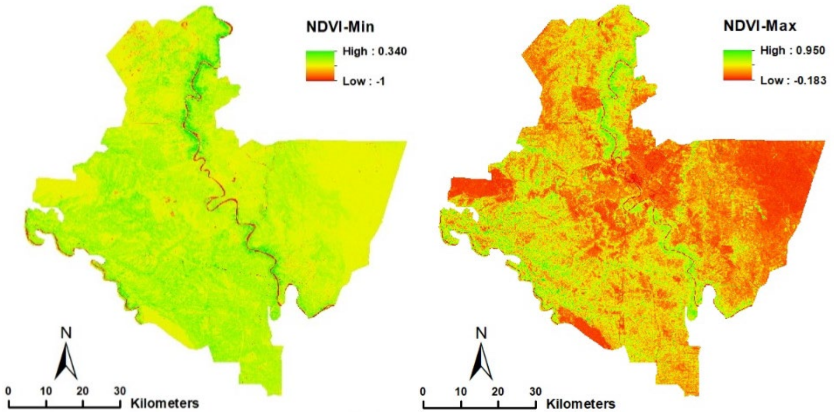

Figure 15: The average minimum and maximum NDVI values for the period 1970–2025

By applying the formula (1) to compute VCI values across the time series from 1970 to 2025 and categorising them based on the drought categories (Table 2), we can in turn generate the spatio-temporal pattern of drought affecting the administrative land of Baghdad. What emerges from the VCI maps is not a linear trajectory of vegetative health across 1970-2025, but a behavioural view in which degradation led to recovery and subsequent relapses. The period starts before 1970, when hydrology appeared stable, the 1970 map shows success, a steady state had been reached and the agricultural belts of Al-Tarmiyah (North) and Al-Yusufiyah (South) were flourishing (VCI > 60%). This stability was not to last long. 1975" not a dry year, but the "precursor" year. The urban core was healthy, but warnings came from Nahrawan (eastern semi-arid district) and on the rain-fed margins of Al-Madain. Drought signs were beginning to emerge (the "Abnormally Dry" label) in 1975. Ignoring the spatial alarm of 1975, the eroding resilience in hydrology was approaching collapse. 1980 and a systemic collapse of the vegetation index appears on the VCI. Extreme Drought (Red) had taken hold and infected the vital western breadbasket of Abu Ghraib and the southerly orchards of Al-Mahmudiya. This represents the continuum of problematic rain signs from a relatively local state of failure (1975) to widespread failure. After the acute crisis of the early 1980s, there was a slow convalescence and volatility. The 1985 map is transitional; it has moved on from being "Extreme Drought" (1980), but recovery was patchy. Northerly districts of Al-Taji were healing and greening-up moderately well, whereas southerly districts were still in "Moderate Drought" and perhaps could not return to full function. This improvement pattern was upended as the 1990s began. The bright 1990 results show being wound back among outer agricultural cover zones more generally, probably due to some climatic influence combined with infrastructural impacts. But the 1990 exuberance gave way to a momentous 1995, arguably the climatic "optimum" of our 5-year process. Instead of isolated belts of covering with a handful of units failing, there is a broad green swathe across the governorate, the anomaly values are peak as well, even in the always-dangerous zones of Quadrant 5 of Radwaniyah and Al-Istiqlal. What occurred is most likely a very desirable coalescence of timely rain and spatially resonant human land elevation. As we turn the century, instability emerges. The direct transition from the lushness of 1995 to major drought in the 2000 map, which shows as severe as in '80, points to savage sensitivity of inter-annual climate variability, especially as we return to deep red pixels in the Abu Ghraib and Latifiya sectors. This phenomenon continued and morphed into 2005, where the pattern has cast around the urban/rural boundary. By 2005 the vegetation in the "Green Belt" surrounding Baghdad was beginning to fragment (Dora, Baghdad Al-Jadida) hinting that anthropogenic pressures were compounding climate risks. The 2010 map closed the decade of scar severity decline near where it started in terms of drought-state: the imagery remained "transitional" to that of 1985; it was still not in peak drought, but the eastern districts of Jisr Diyala and Nahrawan continued to struggle to recover vegetation and remained within Chronic Moderate Drought (Yellow/Orange).

1970

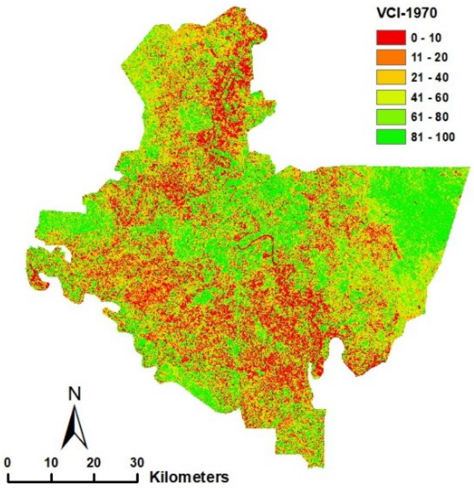

1975

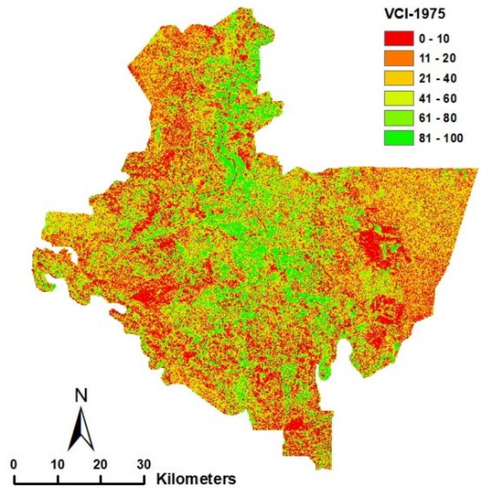

1980

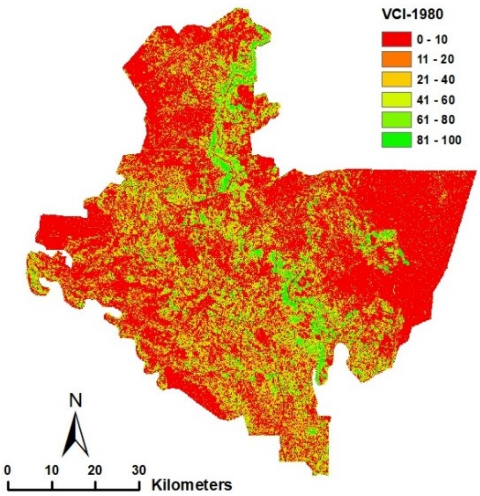

1985

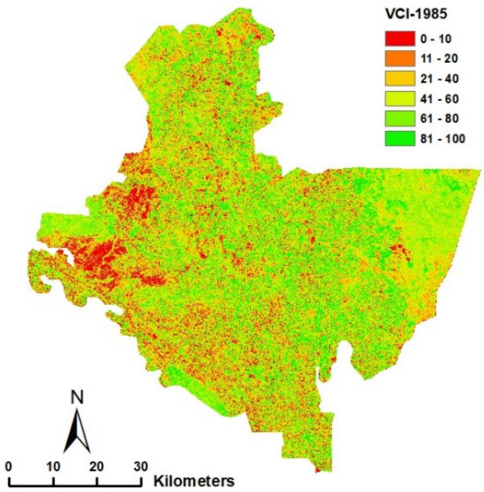

1990

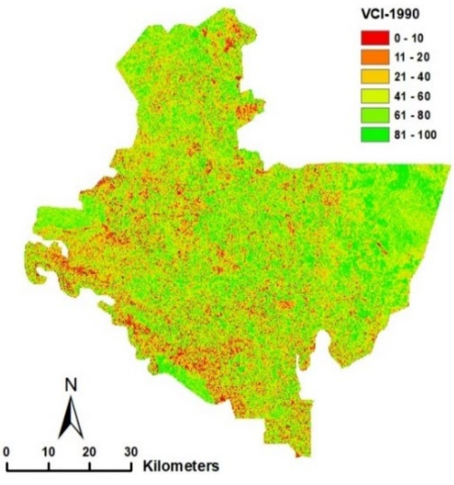

1995

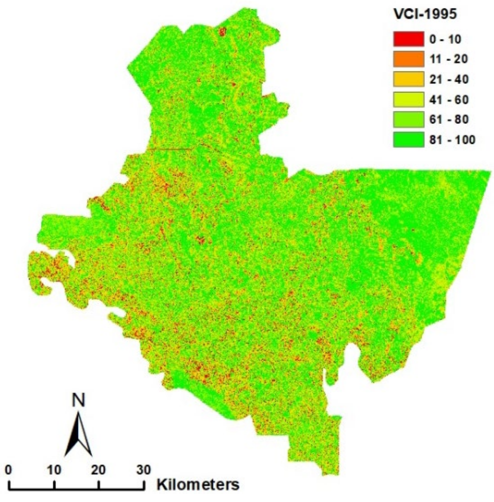

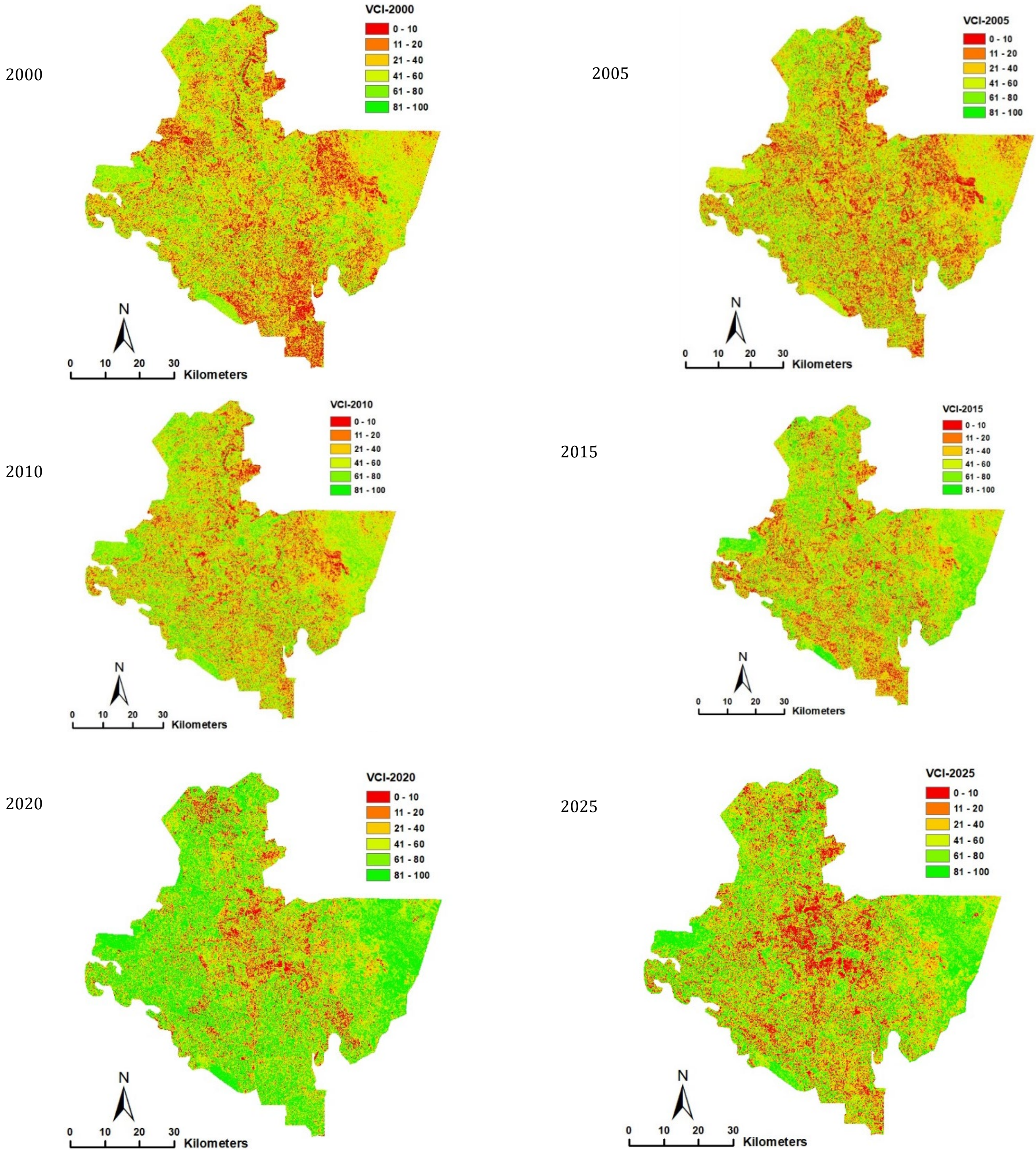

Figure 16: VCI values for Baghdad City, Iraq over the period from 1970 to 2025

In the more recent epochs, a differential response presents; a "mosaic" pattern from 2015 triangulates the agricultural land use; health of vegetation in Al-Taji and the banks of northern riverbanks "patchy", consistent with seasonal irregularity. 2020 however, is a year of "resilience", validating sensitivity of VCI to seasonal precipitation anomalies, 2020 map shows a recovery of VCI values (Green) across the Al-Rasheed and Al-Latifiya districts, on the whole allying to one of the healthiest vegetative states seen in that area between the year 2005. This is not sustained however, and looking further ahead into the twentyfirst century, predictions for 2025 should concern us. Anticipating cyclical impacts in extending this analysis a stated concern is - “A repeat of the conditions observed during the cyclical droughts of 1980 and 2000 is likely”. The 2025 map presumably reflects a change of condition underscoring collapse of the southern horticulture zones and the frontier of "irrigated" land southwest to Khadriya. This pattern vividly warns, without ascertainable countermeasures, the resilience induced in 2020 will be eroded in the face of long-term climatic aridity. Accompanied to judgment of vegetative drought stress via the VCI, is the factor of surface water dynamics giving a focal marker; how much is available and what condition is it in. Water itself is the prime limiting conducive to both agricultural hardiness internally via VCI analytical assessment, propelling the natural ecosystem in "Baghdad" externally. The extent and volumetrics of the hydrological resource is quite changeable, susceptible to the predilection of climatic and anthropogenic variability as to healthy vegetation. Quantifiably remote sensing obtainable then provides a ready means of intervention to account, yet extracting precise hydrological volume offers spectral modelling seriously to indivisible and convoluted semi-arid terrain regions. The (EWI) was chosen to delineate surface water bodies primarily, as it can effectively suppress background noise from urban and soil surfaces, unlike typical models. This makes it ideally suited to resolving the complex water networks of Baghdad. The aim of the EWI is to convert the continuous spectral data to categorical maps explicitly differentiating Emerged Water Region (EWR) from Non-Emerged Water Region (NO–EWR). This binary classification will also serve in tracing the growth and decline of the Tigris River, its tributaries and wetlands over the time range of our study. To assess the spatiotemporal behavior of surface water, the EWI was calculated for the entire time-series from 1970 to 2025 with a 5-year interval to allow us to directly tie-in the cycles of drought we have seen in the VCI to their approximate time of occurrence in the period. Again, the approach was to execute the EWI algorithm in a Geographic Information System (GIS) through its raster calculation function and on generating the all-important index values, applying a threshold of our choice to extract water features from the dry land as seen in the actual images. The resultant images were merely reclassified into their EWR and NO–EWRs. This is seen in, which corroborates the ability of the EWI to extract surface water from Landsat imagery in our work with a hydrological perspective to the vegetation based assessment they produced from the VCI.

1970

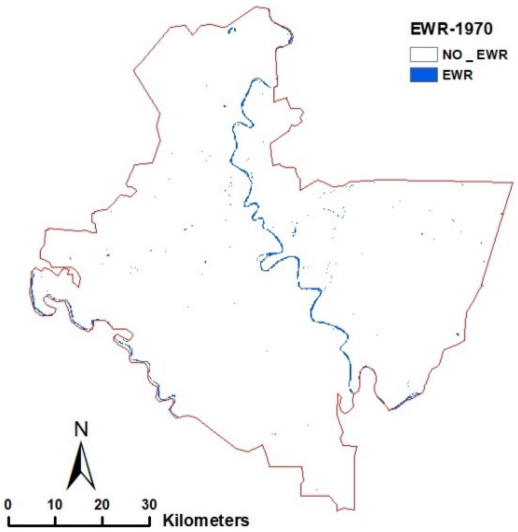

1975

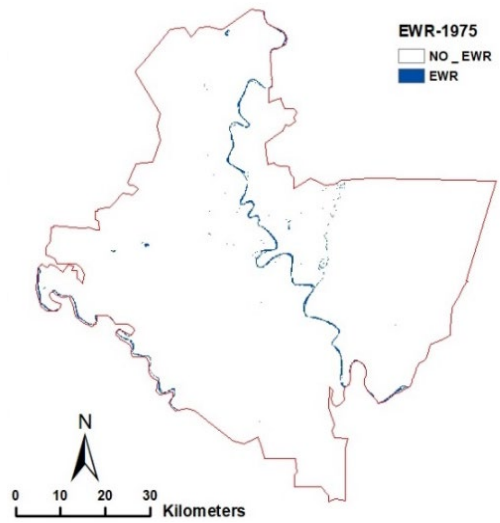

1980

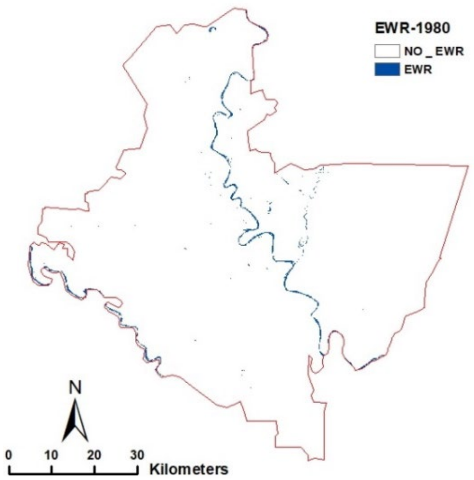

1985

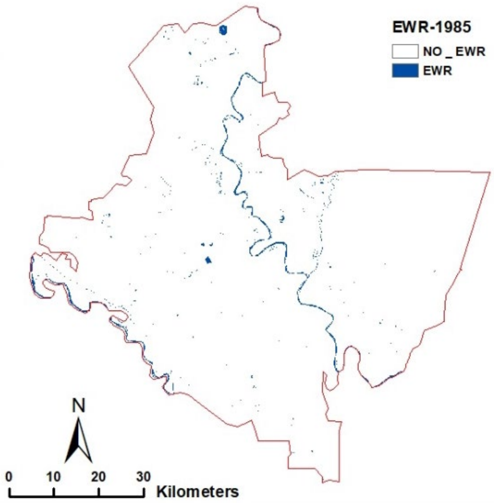

1990

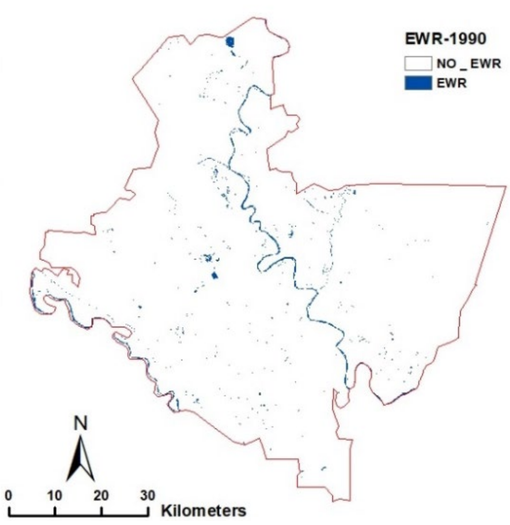

1995

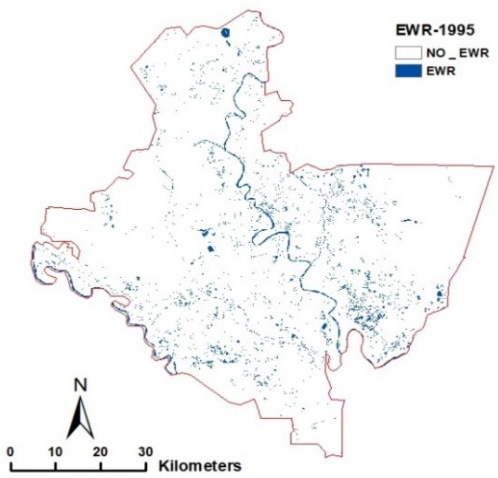

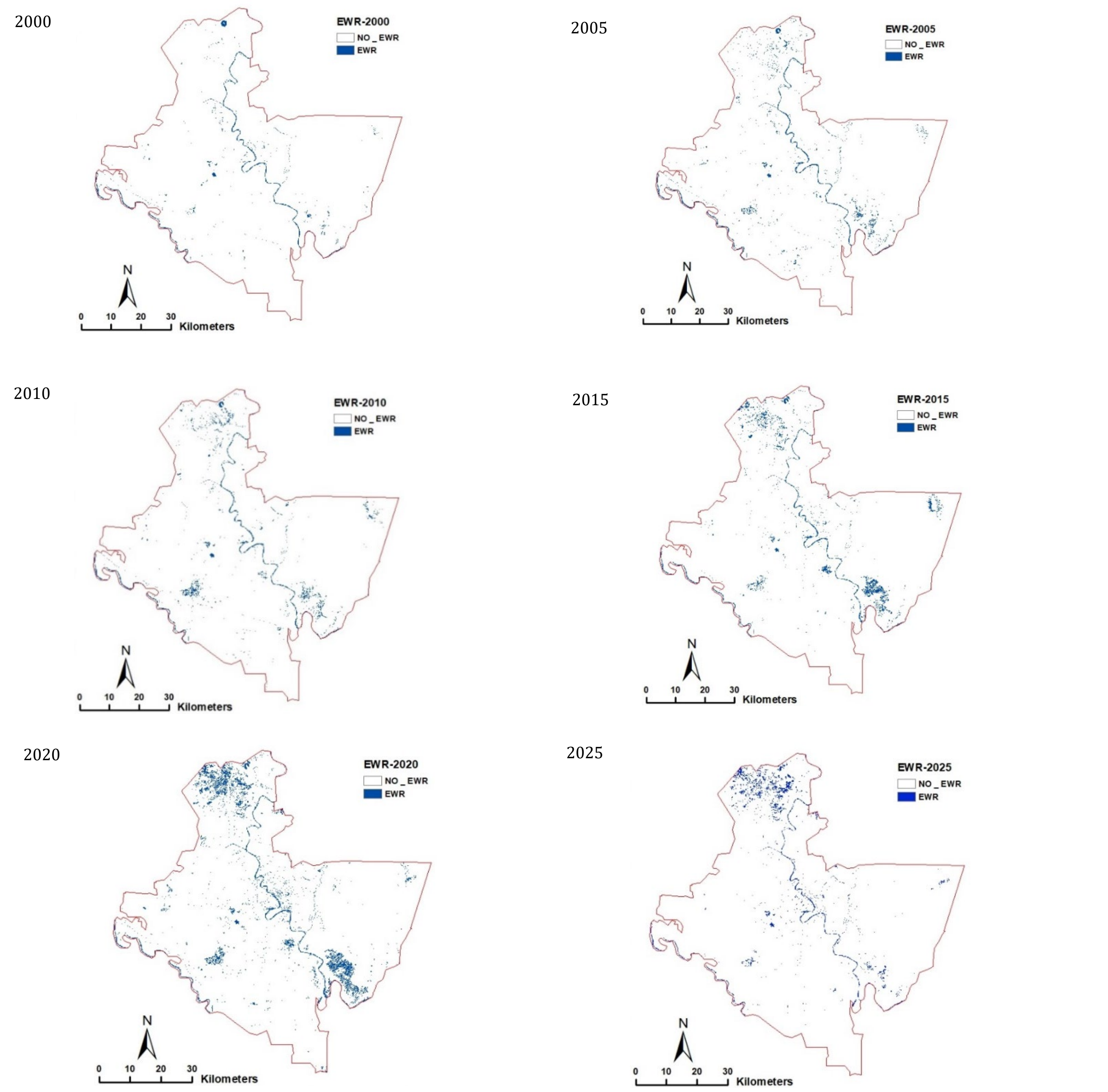

Figure 17: Extracted surface water bodies (EWR) for Baghdad City, Iraq over the period from 1970 to 2025

The (EWI) applied to the continuous Landsat time series produced a highly spatially precise classified assessment of the area studied (EWR) and (NO-EWR). The resultant temporal evolution reveals a strong, linear relationship between the extent of surface water, and the trends identified in the VCI vegetation health study. The determined baseline for 1970 depicts the Tigris River in a vigorous hydrological state of equilibrium, with a large main channel and apparent connectivity between secondary water courses. This resilience began to falter by 1975, exhibiting a distinct narrowing of the river corridor and disappearance of the smaller ephemeral wetlands within the eastern concepts, foreshadowing the crisis. This arid trend continued to build into the year of 1980, the year of maximum stress; referring to the EWI map demonstrates how drastically contracted the EMR is; the Tigris appears really much attenuated, and apparent peripheral wetlands in Nahrawan and Abu Ghraib are practically invisible. The absence of availability of surface water explains the reading of "Extreme Drought" in the vegetation study; discontinuity of the river and the floodplain deprived agricultural land of received irrigation. After the deficit of the early eighties, the area entered into a slow and tortuous recovery of hydrology. The map for 1985 is approaching re-stabilization, although tributary networks remain broken, a reflection of the "Moderate Drought" status of the vegetation. 1990 instability continues in the EWI, which suggests it remained a struggle to expand water to the distal agricultural areas compared to evaporation rates versus regulated flow from upstream, though mid-decade a great rebound appears. 1995 is the optimum - 96's "Hydrological Optimum" where the EWR widened to its fullest extent and at this time the Army Canal and Al-Latifiya's irrigation networks are clear blue lines in the image. This connective tissue helps explain the verdant cover where VCI fades toward the edge. They are not to last, the climate cycle kicked in and 2000 is showing a recession. The EWI now crowds and isolates the river channel from the landscape, in fact it mirrors scarcity found in 1980. The 2005 map captures, fittingly enough, where the low was, it is a low point in the current age and peripheral water as seen in 1995 was gone, leaving the "Green Belt" with no primary water source to stabilize it. 2010 returned an EWR slightly and tepidly recovering in the main channel, but secondary irrigation grids never again recovered, leaving eastern districts of the city in perennial states of crisis. And an interesting capture in the modern state, the EWI for 2015 is indicative of a fragmented system, the northern Taji sector has intermittent canals, a breakout of patchy health for the locus. Yet the next year came, 2020, and is rewarding in the manner of almost an explosion of growth at least during the capture - where it looks to render a more complete state as noted by the EWR "expanding, notably, in the southern meanders of the Tigris". One example of improvement in connectivity in the water network in 2020 compared to the previous decade is that the people received water consistently, which triggered the "Green" recovery visible in VCI maps. Alarmingly, the projection for 2025 looks worse forecasting a contraction of EMR resembling extremes of 1980 and 2000. The river spokes contract to their minimum width and peripheral canals are too faint to register, providing the physical mechanism for the predicted "Severe Drought" and affirming that the ecological health of Baghdad relies on the waxing and waning of surface water network.

5. Conclusions

Beyond any other natural disaster, drought limits the sustainable production of food, disturbs ecological equilibrium, especially in arid zones like Baghdad where the landform is intimately attuned to the rhythms of the Tigris River. In this study, we proposed and implemented a rapid and precise remote sensing approach to track the spatiotemporal changes of this dual problem, vegetational stress and water scarcity, over a several decade time series. By combining the Vegetation Condition Index (VCI) and the (EWI) into a single continuous Landsat time series from 1970 - 2025 - the spatio-temporal relation of how this ecosystem responds to climatic fluctuation is quantitatively established. Our approach revealed that whereas VCI gives a suitable categorization of the intensity of agricultural drought, the EWI gives a superior indicator value for binary classification, effectively classifying EWR from a dry land. Together they exhibit a direct causal relation - the state of the "Green Belt" in Baghdad is immediately contingent upon the spread and continuity of the surface water network. Our longitudinal study revealed that Baghdad's environmental fate is held not to be a linear entropy, rather a perceptible cyclical rhythm of degradation and rejuvenation, with major drought events appearing every 20 to 25 years. The model identified 1980 as a catastrophic stress year with failure in the vigor of vegetation and a dramatic contraction of river channel; the severe water deficit was repeated in the 2000–05 epoch, where isolation of the Tigris from the floodplain in districts such as Abu Ghraib, Al-Madain, is analogous to that of the extreme scarcity of the 1980s. On the flip side, the years 1995 and 2020 are labeled periods of 'hydrological optimum'. Favorable precipitation and being privy to an increase in upstream flows led to a general expansion of the EMR and a risk free explosion of green vegetation. But this resilience does not last long. Most worrying is the prediction of 2025 where the findings appear to be aligning with a new nadir of dryness. VCI and EWI appear to be predicting a return of the "Severe" to "Extreme" drought conditions seen in 1980, where the drying of the peripheral irrigation arteries in Al-Latifiya, Al-Tarmiyah looks set to be repeated. "Our conclusion is that reduced precipitation and contraction of flow have been the main drivers of the crises. On the evidence it appears that unless action is taken to modernize the water supply infrastructure, the region is condemned to experiencing a repeat of cycles." This research is crucial especially being an operational reference for city planners water resources managers in Iraq.

References

Agarwal, V., Vishvendra Raj Singh, B., Marsh, S., Qin, Z., Sen, A., and Kulhari, K., 2025. Integrated Remote Sensing for Enhanced Drought Assessment: A Multi-Index Approach in Rajasthan, India. Earth and Space Science, 12(2), e2024EA003639.

Al-Adili, A., 1998. Geotechnical evaluation of Baghdad soil subsidence and their treatments. University of Baghdad.

Al-Ansari, N., Knutsson, S., and Ali, A., 2012. Restoring the garden of Eden, Iraq. Journal of Earth Sciences and Geotechnical Engineering, 2(1), Pp. 53-88.

Ali, Z. R., and Muhaimeed, A. S., 2016. The study of temporal changes on land cover/land use prevailing in Baghdad governorate using RS and GIS. The Iraqi Journal of Agricultural Sciences, 47(3), Pp. 846-855.

Allen, G. H., and Pavelsky, T. M., 2018. Global extent of rivers and streams. Science, 361(6402), Pp. 585-588.

Aznarez, C., Jimeno-Sáez, P., López-Ballesteros, A., Pacheco, J. P., and Senent-Aparicio, J., 2021. Analysing the impact of climate change on hydrological ecosystem services in Laguna del Sauce (Uruguay) using the SWAT model and remote sensing data. Remote Sensing, 13(10), 2014.

Cao, H., Han, L., Liu, Z., and Li, L., 2021. Monitoring and driving force analysis of spatial and temporal change of water area of Hongjiannao Lake from 1973 to 2019. Ecological Informatics, 61, 101230.

Danaher, T., and Collett, L., 2006. Development, optimisation and multi-temporal application of a simple Landsat based water index. Proceedings of the 13th Australasian Remote Sensing and Photogrammetry Conference,

FAO., 2018. Disasters Causing Billions in Agricultural Losses, with Drought Leading the Way, FAO in Geneva, Organización de Las Naciones Unidas Para La Alimentación y La Agricultura. 2018. Available online: https://www.fao.org/geneva/news/detail/es/c/1109572/ (Accessed 10 October, 2023).

Feyisa, G. L., Meilby, H., Fensholt, R., and Proud, S. R., 2014. Automated Water Extraction Index: A new technique for surface water mapping using Landsat imagery. Remote sensing of Environment, 140, Pp. 23-35.

Garrido-Rubio, J., Calera, A., Arellano, I., Belmonte, M., Fraile, L., Ortega, T., Bravo, R., and González-Piqueras, J., 2020. Evaluation of remote sensing-based irrigation water accounting at river basin district management scale. Remote Sensing, 12(19), Pp. 3187.

Gaznayee, H. A. A., Al-Quraishi, A. M. F., and Al-Sulttani, A. H. A., 2021. Drought spatiotemporal characteristics based on a vegetation condition index in Erbil, Kurdistan Region, Iraq. Iraqi Journal of Science, Pp. 4545-4556.

Gaznayee, H., and Al-Quraishi, A. M. F., 2019. Analysis of agricultural drought's severity and impacts in Erbil Province, the Iraqi Kurdistan region based on time series NDVI and TCI indices for 1998 through 2017. Jour of Adv Research in Dynamical and Control Systems, 11(11), Pp. 287-297.

Gitelson, A. A., Kogan, F., Zakarin, E., Spivak, L., and Lebed, L., 1998. Using AVHRR data for quantitive estimation of vegetation conditions: Calibration and validation. Advances in space research, 22(5), Pp. 673-676.

Haitham, M., Mustafa, M. T., and Ismail, A. H., 2024. Accuracy Assessment of Land Use/Land Cover Indices for Al-Rusafa in Baghdad Governorate by Remote Sensing Technology and GIS. IOP Conference Series: Earth and Environmental Science,

Hashim, B. M., Al Maliki, A., Sultan, M. A., Shahid, S., and Yaseen, Z. M., 2022. Effect of land use land cover changes on land surface temperature during 1984–2020: A case study of Baghdad city using landsat image. Natural Hazards, 112(2), Pp. 1223-1246.

Jassim, S. Z., and Goff, J. C., 2006. Geology of Iraq. DOLIN, sro, distributed by Geological Society of London.

Ji, L., and Peters, A. J., 2003. Assessing vegetation response to drought in the northern Great Plains using vegetation and drought indices. Remote sensing of Environment, 87(1), Pp. 85-98.

Kareem H. H., Alkatib A. A., and Mahdi W. H., 2021. Watershed basins delineation using GIS and Digital Elevation Model (DEM) to the region NI-38-14 Karbala-Al-Najaf Plateau, Iraq. Journal of Physics: Conference Series, 1973 (1), No. 012188.

Kareem, H. H., 2024. Monitoring drought condition through detecting the vegetation condition index at Barry City in Wales, UK using temporal Landsat imageries. International Journal of Water, 16(1), Pp. 23-41.

Kareem, H. H., Attaee, M. H., and Omran, Z. A., 2023. Extraction of the Spatial and Temporal Surface Water Bodies Using High Resolution Remote Sensing Technology at Cardiff City, United Kingdom. Journal of Ecological Engineering, 24(11).

Klymenko, K., and Boychenko, S., 2025. Spatiotemporal Analysis of Vegetation Stress in the Mykhailivskyi and Yelanets Steppes under Climate Aridization (2010–2024). International Conference of Young Professionals «GeoTerrace-2025»,

Kogan, F. N., 1990. Remote sensing of weather impacts on vegetation in non-homogeneous areas. International journal of remote sensing, 11(8), Pp. 1405-1419.

Kogan, F. N., 1995a. Application of vegetation index and brightness temperature for drought detection. Advances in space research, 15(11), Pp. 91-100.

Kogan, F. N., 1995b. Droughts of the late 1980s in the United States as derived from NOAA polar-orbiting satellite data. Bulletin of the American meteorological society, 76(5), Pp. 655-668.

Kogan, F. N., 1997. Global drought watch from space. Bulletin of the American meteorological society, 78(4), Pp. 621-636.

Lawal, S., Hewitson, B., Egbebiyi, T. S., and Adesuyi, A., 2021. On the suitability of using vegetation indices to monitor the response of Africa's terrestrial ecoregions to drought. Science of the Total Environment, 792, 148282.

Lesk, C., Rowhani, P., and Ramankutty, N., 2016. Influence of extreme weather disasters on global crop production. Nature, 529(7584), Pp. 84-87.

Liu, L., Yang, X., Zhou, H., Liu, S., Zhou, L., Li, X., Yang, J., Han, X., and Wu, J., 2018. Evaluating the utility of solar-induced chlorophyll fluorescence for drought monitoring by comparison with NDVI derived from wheat canopy. Science of the Total Environment, 625, Pp. 1208-1217.

Lu, Z., Wang, D., Deng, Z., Shi, Y., Ding, Z., Ning, H., Zhao, H., Zhao, J., Xu, H., and Zhao, X., 2021. Application of red edge band in remote sensing extraction of surface water body: A case study based on GF-6 WFV data in arid area. Hydrology Research, 52(6), Pp. 1526-1541.

Malahlela, O. E., 2016. Inland waterbody mapping: Towards improving discrimination and extraction of inland surface water features. International journal of remote sensing, 37(19), Pp. 4574-4589.

McFeeters, S. K., 1996. The use of the Normalized Difference Water Index (NDWI) in the delineation of open water features. International journal of remote sensing, 17(7), Pp. 1425-1432.

McKee, T. B., Doesken, N. J., and Kleist, J., 1993. The relationship of drought frequency and duration to time scales. Proceedings of the 8th Conference on Applied Climatology,

Nag, T., Mohanty, B., Sahu, C., Panigrahi, G., and Dugal, D. (2024). Evaluating the utility of normalized difference vegetation index (NDVI) and vegetation condition index (VCI) for monitoring drought in Bolangir district of Odisha. International Journal of Research in Agronomy.

Nassrullah, S. A., Ismail, A. H., Al, Q. A.-N. A. K., Al-Zuhairy, M. S., and Farhan, A. A.-R., 2025. Spatial and temporal variations of the water quality of Tigris River in North and South of Baghdad city. IOP Conference Series: Earth and Environmental Science,

Palmer, W. C., 1965. Meteorological drought. US. Weather Bureau Res. Paper, 45, Pp. 1-58.

Papa, F., Crétaux, J.-F., Grippa, M., Robert, E., Trigg, M., Tshimanga, R. M., Kitambo, B., Paris, A., Carr, A., and Fleischmann, A. S., 2022. Water resources in Africa under global change: monitoring surface waters from space. Surveys in Geophysics, 20, Pp. 1-51.

Parente, L., Mesquita, V., Miziara, F., Baumann, L., and Ferreira, L., 2019. Assessing the pasturelands and livestock dynamics in Brazil, from 1985 to 2017: A novel approach based on high spatial resolution imagery and Google Earth Engine cloud computing. Remote sensing of Environment, 232, 111301.

Purnam, K. K., Prasad, A., and Ganasala, P., 2024. Water indices for surface water extraction using geospatial techniques: a brief review. Sustainable Water Resources Management, 10(2), 70.

Quiring, S. M., and Papakryiakou, T. N., 2003. An evaluation of agricultural drought indices for the Canadian prairies. Agricultural and forest meteorology, 118(1-2), Pp. 49-62.

Rhee, J., Im, J., and Carbone, G. J., 2010. Monitoring agricultural drought for arid and humid regions using multi-sensor remote sensing data. Remote sensing of Environment, 114(12), Pp. 2875-2887.

Riebsame, W. E., 2019. Drought and natural resources management in the United States: impacts and implications of the 1987-89 drought. Routledge.

Rouse, J., Haas, R., Schell, J., and Deering, D., 1974. Monitoring Vegetation Systems in the Great Plains with ERTS. NASA Special. Publication, 1.

Sandeep, P., Reddy, G. O., Jegankumar, R., and Kumar, K. A., 2021. Monitoring of agricultural drought in semi-arid ecosystem of Peninsular India through indices derived from time-series CHIRPS and MODIS datasets. Ecological indicators, 121, 107033.

Senhorelo, A. P., Sousa, E. F. d., Santos, A. R. d., Ferrari, J. L., Peluzio, J. B. E., Zanetti, S. S., Carvalho, R. d. C. F., Camargo Filho, C. B., Souza, K. B. d., and Moreira, T. R., 2023. Application of the vegetation condition index in the diagnosis of spatiotemporal distribution of agricultural droughts: A case study concerning the state of Espírito Santo, Southeastern Brazil. Diversity, 15(3), 460.

Shen, Z., Zhang, Q., Singh, V. P., Sun, P., Song, C., and Yu, H., 2019. Agricultural drought monitoring across Inner Mongolia, China: Model development, spatiotemporal patterns and impacts. Journal of Hydrology, 571, Pp. 793-804.

Somasundaram, D., Zhang, F., Ediriweera, S., Wang, S., Li, J., and Zhang, B., 2020. Spatial and temporal changes in surface water area of Sri Lanka over a 30-year period. Remote Sensing, 12(22), 3701.

Song, W., Hu, Q., Liu, S., and Hou, Y., 2025. Decadal spatiotemporal dynamics of surface water bodies in Zhengzhou, China: remote sensing monitoring and analysis of driving factors. Scientific Reports.

Taha, A. M., Ibrahim, I. A., Abduladeem, H., Yassen, M. Q., Ahmed, O. K., and Abdul-Allah, T. N., 2024. Assessing drought conditions in southern Baghdad (1988-2023) using NDVI anomaly and its impact on soil and vegetation. Pakistan Journal of Agricultural Research, 37(3), 241.

Tariq, A., Shu, H., Kuriqi, A., Siddiqui, S., Gagnon, A. S., Lu, L., Linh, N. T. T., and Pham, Q. B., 2021. Characterization of the 2014 indus river flood using hydraulic simulations and satellite images. Remote Sensing, 13(11), 2053.

Tawfik, M. K., and Al-Lami, A. M., 2025. Assessment Of The Impact Of Climate Change On Land Use/Land Cover For Southern Iraq Using Landsat Data. IOP Conference Series: Earth and Environmental Science,

Thi, N. Q., and Van Hung, H., 2024. Space-Time Variability of Drought in Tay Nguyen Provinces, Vietnam Using Satellite-Based Vegetation Time Series from 2000 to 2023: 10.32526/ennrj/22/20240063. Environment and Natural Resources Journal, 22(5), Pp. 437-448.

Van Quang, N., Long, D., Anh, N., and Hai, T., 2021. Administrative capacity of local government in responding to natural disasters in developing countries. J. Hum. Earth Future, 2, Pp. 114-124.

Vinayaraj, P., Imamoglu, N., Nakamura, R., and Oda, A., 2018. Investigation on perceptron learning for water region estimation using large-scale multispectral images. Sensors, 18(12), 4333.

Wenzhe, J., Zhang, L., Chang, Q., Fu, D., Cen, Y., and Tong, Q., 2016. Evaluating an enhanced vegetation condition index (VCI) based on VIUPD for drought monitoring in the continental United States. Remote Sensing, 8(224), Pp. 1-21.

Wu, J., Zhou, L., Liu, M., Zhang, J., Leng, S., and Diao, C., 2013. Establishing and assessing the Integrated Surface Drought Index (ISDI) for agricultural drought monitoring in mid-eastern China. International Journal of Applied Earth Observation and Geoinformation, 23, Pp. 397-410.

Xia, F., and Lv, G., 2024. Evaluation of machine learning algorithm capability for Bosten Lake Wetland classification based on multi-temporal Sentinel-2 data. Ecological Informatics, 84, 102839.

Xu, H. j., Wang, X. p., Zhao, C. y., and Yang, X. m., 2021. Assessing the response of vegetation photosynthesis to meteorological drought across northern China. Land Degradation and Development, 32(1), Pp. 20-34.

Yadav, A. T., MR, A. L., and Subramaniam, M., 2025. Drought Assessment in Karnataka's Western Ghats Using MODIS-Derived Vegetation Condition Index. International Journal of Environmental Sciences, 11(12s), Pp. 400-410.

Yamazaki, D., Trigg, M. A., and Ikeshima, D., 2015. Development of a global~ 90 m water body map using multi-temporal Landsat images. Remote sensing of Environment, 171, Pp. 337-351.

Yan, P., Zhang, Y., Zhang, Y., 2007. A study on information extraction of water enhanced water index (EWI) and GIS system in semi-arid regions with the based noise remove techniques. Remote Sensing, 6, Pp. 62-67.

Zhang, A., and Jia, G., 2013. Monitoring meteorological drought in semiarid regions using multi-sensor microwave remote sensing data. Remote sensing of Environment, 134, Pp. 12-23.